

Surrogate Markers for Glioma Diagnosis: Diffusion Weighted Magnetic Resonance Imaging and Magnetic Resonance Spectroscopy

June 23, 2009

Lars Ewell, Amarjeet Bhullar, Ray Carmody,
Russell Hamilton, Joshua Kim and Baldassarre Stea

Preliminary Studies

MRS

As part of a related Internal Review Board (IRB) approved study¹, a number of patients as well as an MRS phantom have been scanned using multi-voxel MRS. The spherical MRS phantom (diam=20.3cm) contained the three brain metabolites, Cho, Cr and NAA in roughly the same concentrations as a healthy human brain: 3.0 milli-molar(mM), 10.0mM and 12.5mM respectively. The metabolite peaks were fit using a Gaussian function, and the metabolite concentrations and ratios were plotted as a function of voxel location. Figure 5 depicts the phantom with the 7x7 grid superimposed, as well as a sample spectra from voxel 25. The data from these spectra are displayed in Table 2. As can be seen there, although the MRS signal (peak area) for Cho and NAA for different voxels varies by 202 and 215% respectively, the Cho/NAA ratio is constant to within 9%, indicating that the metabolite ratio is relatively insensitive to MRS signal fluctuations. Figure 6 depicts the absolute metabolite fluctuation, as well as the ratio variation as a function of voxel location. Only the central 25 voxels were analyzed. As can be seen in this figure, the absolute metabolite signal (peak area) showed a significant correlation with voxel location, whereas the ratio did not.

For this MRS phantom, our metabolite calculations were in good agreement with the automatic ratios that are calculated via the *Functool* software on the 3T GE Excite MRI machine. However, for patients, the variation in metabolite ratio and peak location was much less predictable. For this reason, we display the MRS data in this form, so as to more accurately represent the ratios. In Figure 7, a healthy volunteer MRS spectra is displayed. In Figure 8, a patient MRS scan is displayed. These data are also displayed in Table 3, similar to Table 2. As can be seen in these data, the volunteer and patient absolute metabolite signals show a variation similar to the phantom. However, the volunteer and especially the patient Cho/NAA

¹see <http://www.u.arizona.edu/~lewell/protocol/index.html>

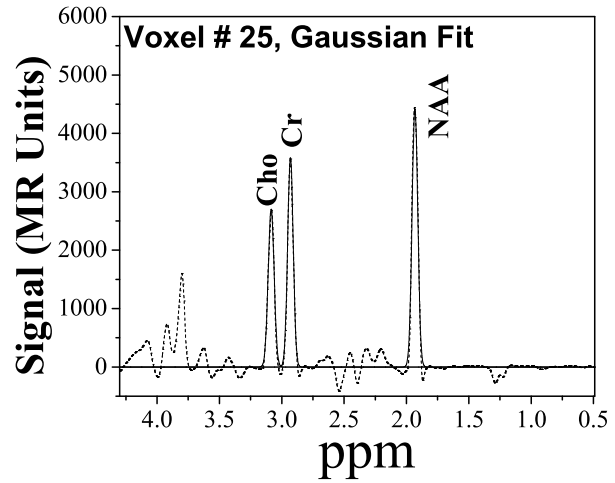
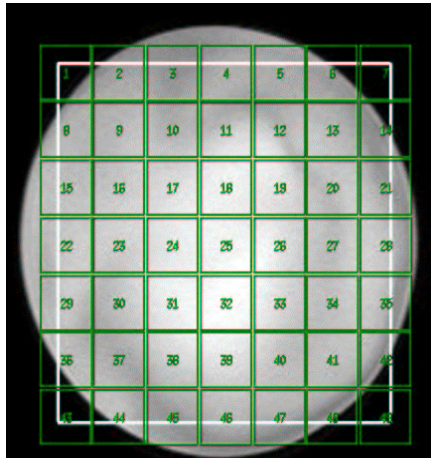


Fig 5: **Left** - An MRI image of the CSI phantom filled with Cho(3.0mM), Cr(10.0mM), and NAA(12.5mM) and a 7x7 grid superimposed.; **Right** - The spectra from voxel number 25. The dashed line is the real spectrum and solid line as Gaussian functions overlapped on respective peaks.

Table 2: Phantom Metabolite Concentration and Ratio Variation

Metabolite-Ratio	Min	Mean	Max	% Variation
Cho	52.7	96.3	159.6	202
NAA	79.4	146.7	250.0	215
Cho/NAA	0.61	0.63	0.67	9.0

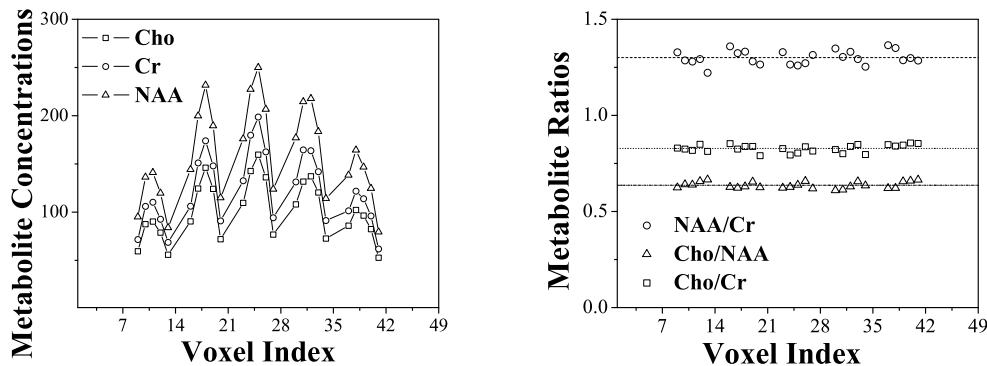


Figure 6: **Left** - Absolute metabolite concentration (peak area) as a function of voxel location. Central voxel (25) has highest concentration. **Right** - Metabolite ratio as a function of voxel location.

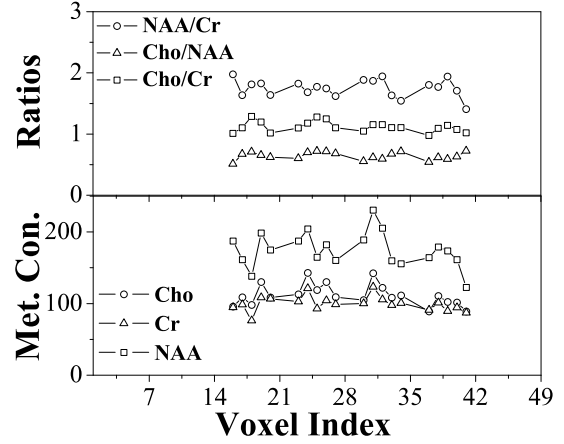
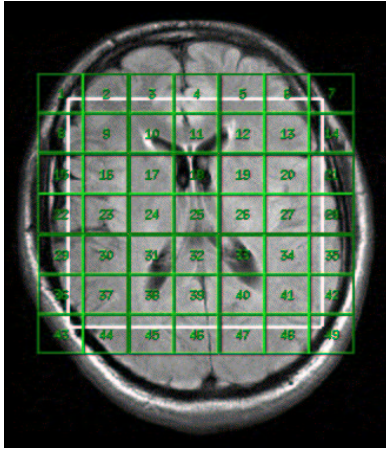


Figure 7: **Left** - Healthy Volunteer MRS scan. **Right** - Metabolite and ratio variation.

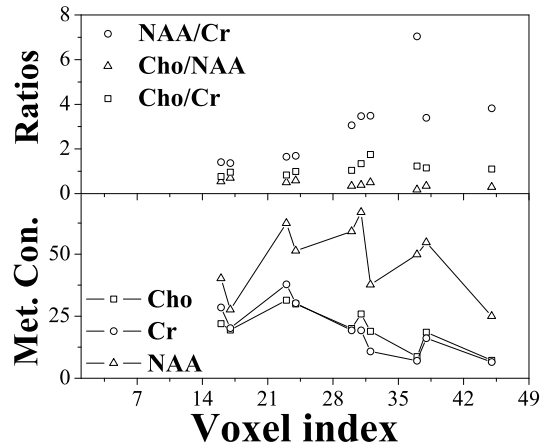
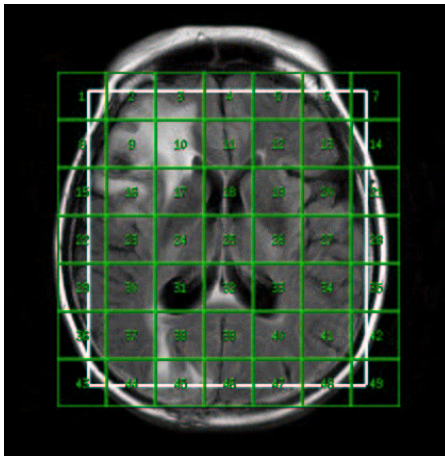


Figure 8: **Left** - Patient MRS scan. **Right** - Metabolite and ratio variation.

Table 3: Patient and Volunteer Metabolite Concentration and Ratio Variation

Person	Metabolite/Ratio	Min	Mean	Max	% Variation
Volunteer	Cho	88.9	111.8	142.8	60.6
Volunteer	NAA	122.6	174.1	230.5	88.0
Volunteer	Cho/NAA	0.51	0.64	0.73	43.1
Patient	Cho	7.20	19.73	31.42	336
Patient	NAA	25.01	50.57	66.88	167
Patient	Cho/NAA	0.18	0.44	0.70	300

ratio exhibits far more variation than the phantom data. In addition to the ratio variation, the background of patient scans add a level of complexity to MRS interpretation. In Figure 9 a patient MRS scan is displayed, along with background. As can be seen in this spectra, a large

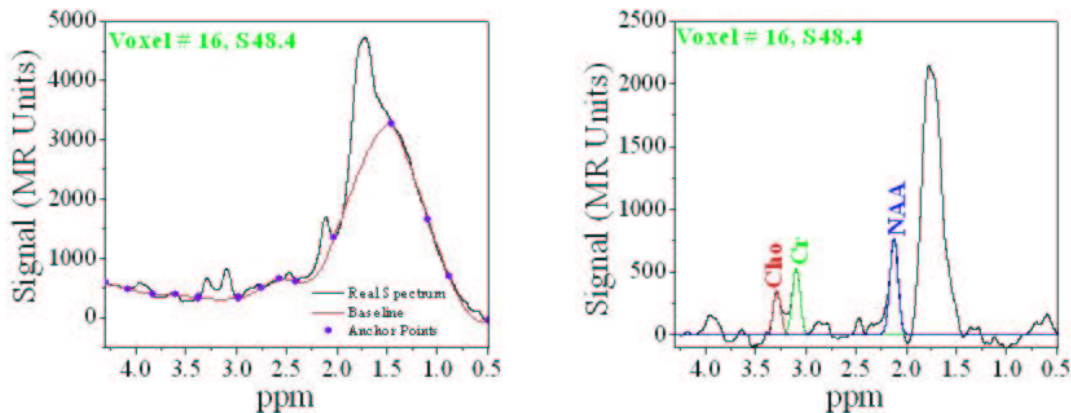


Figure 9: **Left** - Voxel spectra with background(lipid). **Right** - Voxel spectra with background subtracted.

(lipid/lactate) peak adds substantially to the background. To estimate the background, some anchor points are chosen that presumably lie outside the range of the known MRS peaks(left plot). The background is then subtracted, to yield a spectra that is more easily analyzed(right).

ADC

In addition to the MRS scans mentioned above, the same patients also received isotropic Diffusion Weighted MRI (DWMRI) scans as a part of the imaging protocol. These included two different types of diffusion weighting: 1) The most common form of diffusion weighting, echo planar[16]. 2) A more recently developed form of diffusion weighting, radial diffusion[17]. In Figure 10, the lesions of an enrolled patient are displayed. These lesions were longitudinally monitored, using both echo planar and radial diffusion DWMRI scans. Some of the characteristics of the different types of DWMRI scans are displayed in Table 4. The ADC is determined via a plot of the ratio of the log of pixel intensities vs. b-value:

$$\log \frac{I_i}{I_o} = -b_i * ADC \quad (1)$$

where i represents the different b-values of diffusion weighting, and I_i is the corresponding pixel intensities of the lesions in these scans. Error bars are calculated to accommodate the transcription uncertainty, as well as noise[18]. After this uncertainty is quantified, this equation is plotted. A typical plot is shown in Figure 11. As can be seen, the $b=0$ ($i=0$) point has no error bars since in the fraction, the numerator equals the denominator: I_o . Furthermore, since $\log(1) = 0$, there is no intercept. Previous work has demonstrated the importance of uncertainty in the highest b-value[19]. A weighted least squares fit to the data is performed[20], the slope

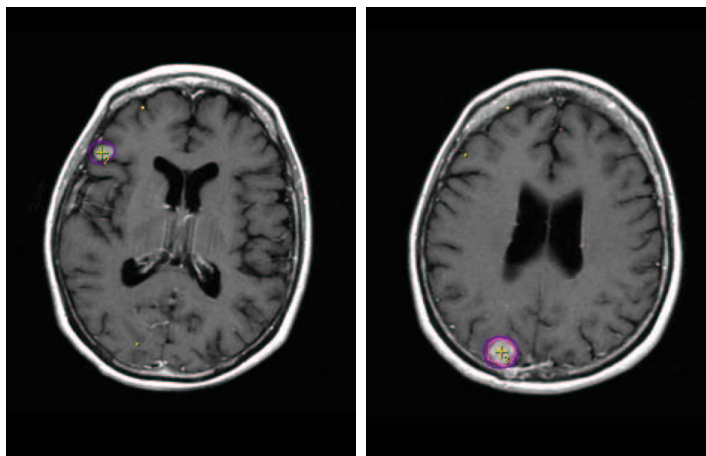


Figure 10: **Left** - Lesion number 2. **Right** - Lesion number 3.

Table 4: DWMRI Scan Characteristics

Scan Type	b-values(s/mm ²)	Slice Spacing(mm)	Slice Thickness(mm)
Echo Planar	0, 1000	7	5
Radical Diffusion	0, 520, 850	7	5

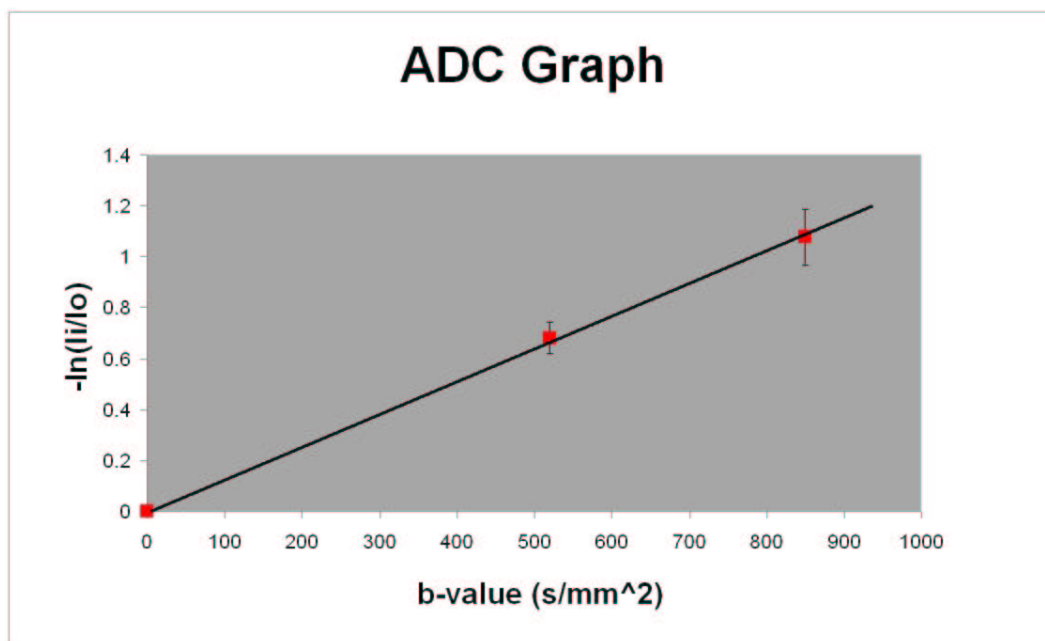


Figure 11: Plot used to determine ADC and Statistical Uncertainty.

of which is the ADC:

$$ADC = \frac{1}{\Delta} \left(\sum_{i=0}^n \frac{b_i}{\sigma_i^2} \log \frac{I_i}{I_0} \right) \quad (2)$$

with

$$\Delta = \sum_{i=0}^n \frac{b_i^2}{\sigma_i^2} \quad (3)$$

where σ_i are the total systematic uncertainties associated with the different log ratios determined above and i ranges over the different b -values of diffusion weighting. Finally, the total (systematic + statistical) uncertainty in the ADC can be written

$$\sigma_{ADC}^2 = 1 / \left(\sum_{i=0}^n \frac{b_i^2}{\sigma_i^2} \right). \quad (4)$$

A plot of the ADC of the two lesions referred to above is show in Figure 12. As can be seen

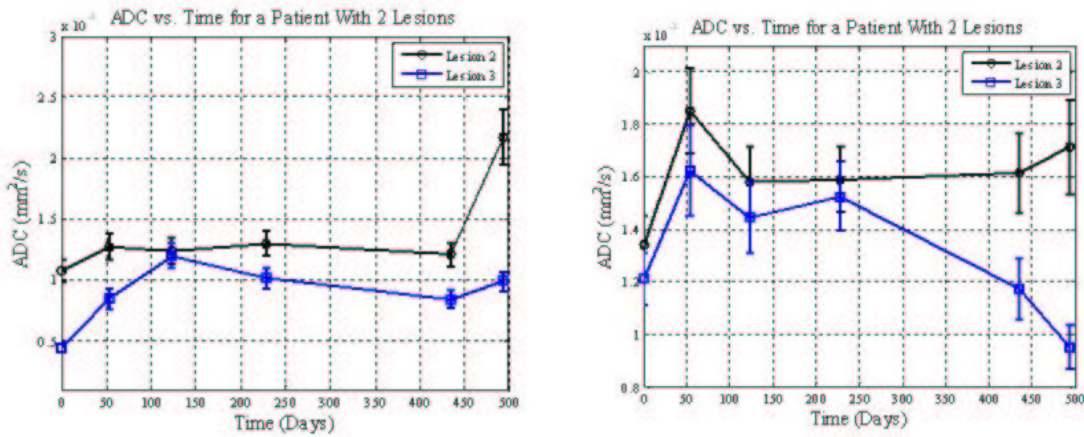


Figure 12: **Left** - Echo Planar ADC vs time. **Right** Radial Diffusion vs time.

in this figure, there is a difference between the two types of diffusion weighting.